Influence of Fe^{2+}-catalysed iron oxide recrystallization on metal cycling

Drew E. Latta*, Christopher A. Gorski† and Michelle M. Scherer‡[1]

*Biosciences Division, Argonne National Laboratory, Argonne, IL 60439, U.S.A., †Environmental Chemistry, Swiss Federal Institute of Aquatic Science and Technology, Eawag, Ueberlandstrasse 133, 8600 Duebendorf, Switzerland, and ‡Department of Civil and Environmental Engineering, University of Iowa, Iowa City, IA 52242, U.S.A.

Abstract

Recent work has indicated that iron (oxyhydr-)oxides are capable of structurally incorporating and releasing metals and nutrients as a result of Fe^{2+}-induced iron oxide recrystallization. In the present paper, we briefly review the current literature examining the mechanisms by which iron oxides recrystallize and summarize how recrystallization affects metal incorporation and release. We also provide new experimental evidence for the Fe^{2+}-induced release of structural manganese from manganese-doped goethite. Currently, the exact mechanism(s) for Fe^{2+}-induced recrystallization remain elusive, although they are likely to be both oxide- and metal-dependent. We conclude by discussing some future research directions for Fe^{2+}-catalysed iron oxide recrystallization.

Metal incorporation in iron oxides

Natural iron (oxyhydr-)oxides are rarely pure. Instead, they often contain structural trace metal impurities (e.g. [1–3]). For example, natural goethites almost always contain substantial amounts of structural aluminium (up to 33 mol%) despite the smaller atomic size of aluminium, which has been attributed to the ubiquity of both iron and aluminium in the environment and co-mobilization during weathering [1]. Primary mechanisms for structural incorporation of metals into iron oxide lattices include mineral formation, secondary mineralization reactions and weathering [2]. Over the last few years, a new mechanism for structural incorporation and release of metals in iron oxides has emerged that involves Fe^{2+}-catalysed iron oxide recrystallization [2,4–7].

Recrystallization of iron oxides in the presence of Fe^{2+} is readily observed for the least stable iron oxides, which transform to secondary minerals (e.g. the transformation of ferrihydrite to goethite, or lepidocrocite to magnetite [8–11]). The transformation process is thought to involve either topotactic reformation or nucleation and recrystallization (i.e. dissolution and reprecipitation) [8–10,12]. For more stable iron oxides, such as goethite and magnetite, however, aqueous Fe^{2+} does not induce any obvious secondary mineralization reactions and, until recently, Fe^{2+} uptake was viewed as a sorption/desorption reaction at the oxide surface [13–16]. Significant experimental evidence indicates that the reaction of aqueous Fe^{2+} with these more stable iron oxides is quite dynamic. Much of this evidence is based on iron isotope tracer studies that demonstrate significant iron atom exchange and recrystallization [9,17–23]. For a review of these studies and the emergence of a revised conceptual model for Fe^{2+} sorption on iron oxides, see [24].

In the present paper, we provide a brief overview of the evidence and possible mechanisms of Fe^{2+}-catalysed iron oxide recrystallization in the absence of secondary transformations and summarize recent findings on metal incorporation and/or release during recrystallization. We also present some new results demonstrating Mn^{2+} release from goethite in the presence of aqueous Fe^{2+} and provide some closing remarks on future research directions for Fe^{2+}-catalysed iron oxide recrystallization.

Fe^{2+}-catalysed iron oxide recrystallization of goethite, haematite and magnetite

There were some clear early indications in the literature that the reaction of aqueous Fe^{2+} with the more stable iron oxides, such as goethite, haematite and magnetite, was more dynamic than a simple adsorption reaction. For example, Tronc et al. [25] examined the uptake of Fe^{2+}, Co^{2+} and Ni^{2+} on magnetite, and saw that three times as much Fe^{2+} sorbed on the magnetite than Co^{2+} or Ni^{2+}, suggesting that Fe^{2+} sorption was not controlled by the availability of reactive surface sites. A similar observation was later made for haematite reacted with Fe^{2+} and other metal cations [26,27]. Coughlin and Stone [28] examined the competitive sorption of Fe^{2+} with other metals on goethite, and found that the presence of Fe^{2+} increased Co^{2+}, Ni^{2+} and Cu^{2+} uptake. These authors hypothesized that the Fe^{2+} taken up from solution formed a mixed-valent phase at the goethite surface, which altered the sorptive capacity of the goethite. Later work using spectroscopic techniques confirmed this hypothesis, and demonstrated that, when Fe^{2+} was taken up by an iron oxide, it became oxidized to Fe^{3+} and transferred the electron into the underlying oxide, resulting in homoepitaxial mineral growth (i.e. haematite grew on haematite, goethite grew on goethite, etc.) [29–34].

Although spectroscopic techniques provided clear evidence for electron transfer between sorbed Fe^{2+} and structural Fe^{3+} in the bulk oxides, there was still little indication that significant atom exchange or recrystallization was occurring. Iron isotope tracer studies provided some of the most compelling evidence regarding the dynamic nature of these more stable iron oxides in the presence of aqueous Fe^{2+}. One of the first studies to use isotopes to demonstrate iron atom exchange between aqueous Fe^{2+} and goethite and haematite was the ^{55}Fe work by Pedersen et al. [9], which demonstrated the release of ^{55}Fe from ^{55}Fe-doped iron oxides after reaction with aqueous Fe^{2+}. After 15 days, isotopic mixing was observed for ferrihydrite (∼100%), lepidocrocite (∼35–70%) and goethite (∼12%). Interestingly, negligible mixing was observed for haematite (<1%). Subsequent studies with enriched aqueous ^{57}Fe tracer studies have observed extensive atom exchange for both goethite (∼100%) and magnetite (∼55%) [6,24,35]. Despite the extensive exchange observed in these studies with magnetite and goethite, there were no observable structural changes, which is somewhat remarkable considering that a substantial number of Fe–O bonds in the particles must have been broken and reformed to reach extensive or complete mixing.

How such substantial mixing can occur, as required by the isotopic data, without any observable changes in the oxide is a fascinating question. Some potential explanations we have presented previously and have been discussed in the literature include: (i) solid-state diffusion of iron atoms through the bulk oxide lattice, (ii) diffusion of iron atoms through micropores in the oxide structure (i.e. 'pore diffusion'), and (iii) bulk electron conduction through the mineral structure coupling oxidative sorption at one site with reductive dissolution at another site (e.g. 'the redox-driven conveyor belt model') [4,24,35,36]. Solid-state diffusion has been ruled out in the past as a likely mechanism because reported iron diffusion rates in iron oxides are too low to explain the observed kinetics of iron atom exchange (e.g. for goethite, estimates of diffusion time at room temperature would take millions of years) [9,35]. In magnetite, however, solid-state iron diffusion rates are much higher, and we have recently noted that solid-state diffusion is a viable explanation for Fe^{2+}-catalysed recrystallization of magnetite observed over several days [6].

Evidence for the bulk conduction mechanism comes from work with haematite where Fe^{2+} has been shown to preferentially sorb and oxidize at the (00l) crystalline faces, whereas reductive dissolution occurs at the (hk0) faces [34,37]. For haematite, the growth of haematite pyramids at (00l) and formation of dissolution pits at (hk0), coupled with the measured potential difference between the two faces, provide a compelling argument for bulk conduction. For other oxides, however, such as goethite and magnetite, where there is no observed change in the oxide particles during recrystallization, it is more difficult to invoke site to site potential differences as a driving force for exchange.

Pore diffusion is perhaps one of the most difficult hypotheses to assess as a potential mechanism for Fe^{2+}-catalysed iron atom exchange. Micropores have been hypothesized to allow for metal migration from bulk solution to deep inside the oxide [38–40]. Along the same lines as pore diffusion, pore formation is another interesting hypothesis often invoked to explain microscopic observations of mineral-replacement reactions where the particle maintains its bulk geometry. The pore-formation hypothesis proposes that a 'front' of mineral transformation moves through the entire particle, starting at the surface and moving inwards ([41] and references therein). During this process, micropores are created within the crystal lattice that are capable of transporting fresh Fe^{2+} from solution to the interior and flushing out structural iron into the bulk solution. A mechanism such as this would be consistent with the lack of particle change observed for oxides such as goethite and magnetite. Currently, there is little experimental evidence available to support or refute this as a potential mechanism to explain Fe^{2+}-catalysed iron atom exchange.

Metal cycling during Fe^{2+}-catalysed iron oxide recrystallization

Although the mechanism of how Fe^{2+}-catalysed iron atom exchange occurs in each oxide is still somewhat unclear, both release of structurally incorporated metals and incorporation of metals from the dissolved phase into the oxide structure have been observed in the presence of aqueous Fe^{2+}, suggesting that metal cycling is linked to Fe^{2+}-catalysed iron oxide recrystallization. Metal cycling in the presence of Fe^{2+} has been observed for ferrihydrite, lepidocrocite, schwertmannite, goethite, haematite and magnetite, and is summarized in Table 1. X-ray spectroscopies [EDX (energy-dispersive X-ray analysis), XAS (X-ray absorption spectroscopy) and XMCD (X-ray magnetic circular dichroism)] and X-ray diffraction have also revealed incorporation of several metals (e.g. chromium, cobalt, nickel, manganese, strontium and arsenic) in magnetite, goethite and siderite during dissimilatory iron reduction of oxide suspensions containing both sorbed and co-precipitated metals, probably due to Fe^{2+}-catalysed transformation [42–46]. Note, however, that we have chosen to include only abiotic studies in Table 1, as the factors that control product distribution in microbial secondary mineralization reactions are complex and include a large number of parameters (Fe^{2+} production rates, biomass loadings, anions present, etc. [47]) that are beyond the scope of the present review. Below we provide brief overviews of metal cycling during Fe^{2+}-catalysed iron oxide recrystallization for each oxide.

Ferrihydrite and lepidocrocite

As some of the less stable iron oxides, ferrihydrite and lepidocrocite undergo clear transformations to secondary minerals when reacted with Fe^{2+} (e.g. [8–10,23]), and several studies have shown that metal substitution occurs when other metals are present (Table 1). Early work by Jang et al. [48] focused on transformation of ferrihydrite in the presence of

Table 1 | Studies of metal uptake and release from iron oxides in the presence of aqueous Fe^{2+}

Oxide	Metal	Atomic radius (Å)*†	Note	Reference(s)
Ferrihydrite	Cu^{2+}	0.73	Incorporation‡	[48]
	Zn^{2+}	0.740	Incorporation‡	[48]
	As^{5+}	0.335	Incorporation‡	[7]
	U^{5+}/U^{6+}	0.76/0.73	Incorporation‡	[5,50]
Lepidocrocite	As^{5+}	0.335	Incorporation‡	[7]
Goethite	Mn^{2+}	0.830	Release	D.E. Latta, C.A. Gorski and M.M. Scherer, our study
	Co^{2+}	0.745	Incorporation	[28]
	Ni^{2+}	0.690	Incorporation	[28]
			Release	[4]
	Cu^{2+}	0.73	Incorporation	[28]
	Zn^{2+}	0.740	Release	[4]
	As^{5+}	0.335	No incorporation	[56]
	Tc^{4+}	0.645	Incorporation	[55]
			Release	[55]
	Pb^{2+}	1.19	No incorporation§	[28]
Haematite	Ni^{2+}	0.690	No incorporation§	[52]
			Release	[4]
	Co^{2+}	0.745	No incorporation§	[52]
	Zn^{2+}	0.740	No incorporation§	[52]
			Release	[4]
	As^{5+}	0.335	No incorporation§	[56]
	Cd^{2+}	0.95	No incorporation§	[52]
Magnetite	Co^{2+}	0.745	Release	[6]
	Cr^{3+}	0.615	Incorporation	[53]

*Atomic radii taken from [71]. All radii are for octahedral co-ordination and high-spin electronic state when applicable, except for As^{5+} (four-co-ordinate).

†For comparison, the atomic radius of Fe^{2+} is 0.780 Å and that of Fe^{3+} is 0.645 Å.

‡Secondary transformation of the iron oxide was observed.

§Concluded from metal-uptake behaviour.

divalent metals (copper and zinc) and Fe^{2+}. In the presence of the divalent metals, Mössbauer spectroscopy indicated the formation of Fe^{2+}-deficient magnetite possibly due to the substitution of structural Fe^{2+} by Me^{2+} in magnetite [48]. Incorporation of the transition metals into the inverse-spinel structure of magnetite can be readily explained by the similar ionic radii of the metals (Table 1) and because many of the transition metals form binary or ternary oxide spinels with or without iron [49]. Incorporation of As^{5+} into lepidocrocite and ferrihydrite reacted with Fe^{2+} has also been suggested on the basis of incomplete recoveries of As^{5+} with sequential chemical extractions [7]. More recently, secondary mineralization of ferrihydrite in the presence of $U^{VI}O_2^{2+}$, under some conditions, resulted in incorporation of an oxidation-resistant form of uranium (U^{5+} and/or U^{6+}) into the structure of goethite and, possibly, magnetite based on XAS [5,50]. Incorporation of metals into secondary iron minerals formed after reaction of ferrihydrite and lepidocrocite is relatively easy to envisage, as the secondary transformations suggest significant dissolution and reprecipitation occurs, leading to both significant iron atom exchange and metal incorporation [8,23,44,45,51].

Haematite

Unlike ferrihydrite and lepidocrocite, reacting haematite with Fe^{2+} does not result in any observable transformation to a secondary mineral. There is compelling evidence from AFM (atomic force microscopy) and SEM (scanning electron microscopy) images, as well as X-ray reflectivity measurements, however, that indicates that some recrystallization occurs with preferential dissolution and growth at different crystallographic faces [32,34,37]. In contrast, isotope studies with ^{55}Fe indicate little iron atom exchange between aqueous Fe^{2+} in haematite, making it unclear to what extent Fe^{2+}-catalysed iron atom exchange occurs [9]. Early studies with haematite exposed to both Fe^{2+} and several divalent metals indicated little incorporation of cadmium, zinc, nickel and cobalt, as all metals except for Fe^{2+} were recovered with 0.5 M HCl extractions [27,52]. More recently, however, XAS results suggest incorporation of Ni^{2+} into haematite exposed to Fe^{2+} based on the local co-ordination environment around nickel atoms being similar to those in nickel-substituted haematite [36]. In addition, release of nickel and zinc from nickel- and zinc-substituted haematite was also observed during reaction with Fe^{2+} [4,36] (Figure 1). Rates and extents of metal release were dependent on Fe^{2+} uptake (i.e.

Figure 1 | Rates of metal release for metal-doped iron oxides exposed to aqueous Fe^{2+} at circumneutral pH values

Control experiments with no aqueous Fe^{2+} resulted in negligible metal release in all studies (not shown). Based on data taken from [4,6], and manganese release data from Figure 2.
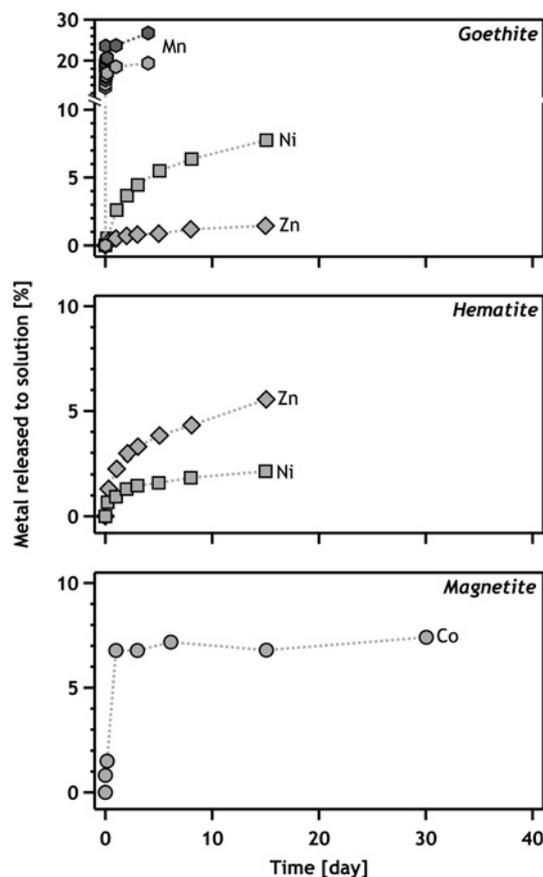
concentration, pH and solids loading) and also on the specific metal.

Magnetite

Several studies have investigated the structural incorporation of metals into the magnetite lattice as a result of secondary mineralization of ferrihydrite and lepidocrocite (see above) as well as due to contaminant reduction (Cr^{3+} [53]), but few have looked at the release of metals directly from magnetite (Table 1). The only work we know of is our recent study comparing Fe^{2+}-catalysed iron atom exchange of magnetite and cobalt-ferrite (a mineral isomorphic with magnetite, where Fe^{2+} is replaced by Co^{2+}) [6]. As shown in Figure 1, approximately 7% of the structural cobalt was released within 1 day when cobalt-ferrite was exposed to Fe^{2+} [6]. In the same study, we used iron isotope tracers to track the fraction of structural iron exchanged and observed approximately 50% iron atom exchange, suggesting that magnetite undergoes substantial recrystallization in the presence of aqueous Fe^{2+} and is likely to be responsible for the cobalt release observed [6].

Goethite

With regard to Fe^{2+}-catalysed iron atom exchange and metal cycling, goethite is probably the most studied iron oxide. Several isotope studies provide clear evidence that Fe^{2+}-catalysed iron atom exchange occurs [9,17,18,35,54] and incorporation of metals in goethite by surface reworking was proposed as far back as 1995 to explain the increase in Cu^{2+}, Ni^{2+} and Co^{2+} uptake by goethite exposed to Fe^{2+} [28]. As with haematite, Frierdich et al. [36] observed incorporation of Ni^{2+} into Fe^{2+}-exposed goethite using XAS, with nickel in a co-ordination environment similar to that of nickel-doped goethite. Incorporation of Tc^{4+} has also been observed with XAS during reaction of goethite with Fe^{2+} solutions [55]. In contrast, XAS indicated that As^{5+} remained sorbed or precipitated as ferrous arsenate rather than being incorporated in goethite during Fe^{2+}-induced recrystallization [56]. Similar to haematite, nickel- and zinc-substituted goethite also released between 2 and 9% of the substituent metals to solution when exposed to Fe^{2+} [4,36] (Figure 1). A comparison between goethite and haematite shows that metal release is not only dependent on the metal and Fe^{2+} uptake, but also on the mineral phase, as zinc-substituted haematite releases more zinc to solution than zinc-substituted goethite, with the trend switched for nickel [4] (Figure 1). Finally, we note that similar magnitudes of release (~5%) occur during microbial respiration of iron in cobalt-substituted goethite [57] (Figure 1).

Few studies have looked at the release of metals such as manganese that can undergo redox reactions with iron. Significant dissolution of both iron and manganese were observed during reduction of manganese-substituted goethite by fermentative bacteria [58]. To determine whether manganese can be released from the manganese-substituted goethite structure during Fe^{2+}-driven recrystallization, we reacted Mn^{3+}-substituted goethites with aqueous Fe^{2+} and measured the release of manganese to solution (Figure 2). In the absence of Fe^{2+}, no release of manganese to solution was observed. In the presence of Fe^{2+}, however, rapid release of manganese was observed in the first 5 min followed by a slower continued release of manganese over the 4 days of the experiment. Interestingly, manganese release and Fe^{2+} uptake were proportional to the amount of manganese incorporated in the goethite, with the 5% manganese-substituted goethite releasing more manganese to solution and taking up more Fe^{2+} than the 2% manganese-substituted goethite (Figure 2). Significantly more release of manganese from doped goethite was observed compared with that of nickel and zinc (Figure 1). The greater release of manganese relative to nickel and zinc may be due to the larger radius of the Mn^{2+} cation formed by reduction of Mn^{3+} by Fe^{2+} (Table 1) (which decreases the favourability for incorporation in goethite). However, anomalous behaviour with Mn^{2+} relative to other transition metals has been observed previously, with little incorporation of manganese into microbial secondary iron mineralization products not following the expected trend with ionic radius [59]. At this point, it is difficult to speculate on why we observed greater release of manganese, because of

Figure 2 | **Manganese release by 2 and 5 mol% manganese-substituted goethite exposed to Fe^{2+}**

Controls are manganese-substituted goethite suspended in buffer without Fe^{2+}. Manganese-substituted goethite was synthesized using procedures described previously [68] that results in structural incorporation of Mn^{3+}. Experimental conditions: $2 \, g \cdot l^{-1}$ manganese-substituted goethite, 25 mM Hepes, 25 mM KBr (pH 7.5) and 1.2 mM $Fe^{2+}Cl_2$. Fe^{2+} was measured with 1,10-phenanthroline [69], and aqueous manganese was measured with formaldoxime [70]. Results are means from duplicate reactors.
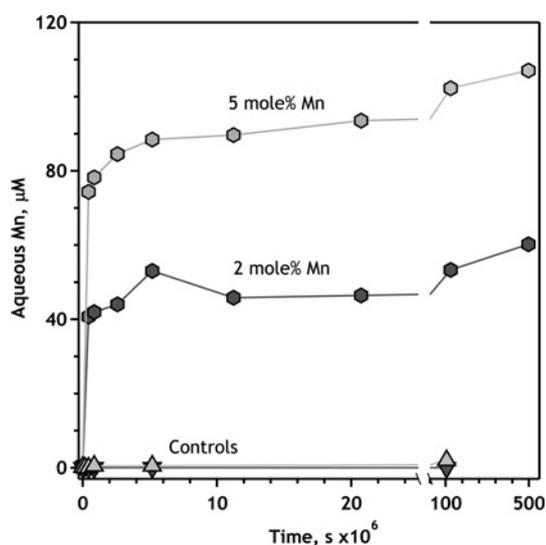
the different affinities of the metals for the goethite surface as well as different experimental conditions.

Closing remarks

Although Fe^{2+}-catalysed iron oxide recrystallization and atom exchange have clearly emerged as new pathways for structural incorporation and release of metals in iron oxides, there remains much that we do not understand. For example, the actual microscopic mechanism of recrystallization and iron atom exchange is still unclear, particularly for the iron oxides that do not undergo transformation to a secondary mineral phase (e.g. goethite, haematite and magnetite). Current working hypotheses for iron atom exchange discussed in the present paper include solid-state diffusion, bulk conduction and pore diffusion. To date, however, there is little definitive evidence to indicate which mechanism is operating with which oxides and how both oxide properties and solution conditions influence these different pathways. For example, incorporation of metals during iron oxide recrystallization may be significantly mediated by elements that hinder oxide transformation or recrystallization, such as aluminium [60], silicate [23] and natural organic matter [23].

On the basis of the limited data available to date (and summarized in the present paper), the amount of metal in the solid and solution phase, as well as the ratio of Fe^{2+} to solid iron appear to play an important role in the

extent of metal release during recrystallization [4]. Other factors that are likely to be important include valence and ionic radius with incorporation likely to be favoured for elements preferring geometries and radii close to those of Fe^{2+} or Fe^{3+} in iron oxides (Table 1). Future work clearly requires atomistic simulations to provide information on the thermodynamic and structural driving forces for metal incorporation and release (e.g. [61,62]). From a more phenomenological standpoint, possible models that may be of use to predict Fe^{2+}-driven metal cycling are those based on a partition coefficient (K_d or D), such as the Henderson–Kracek [63] and Doerner–Hoskin [64] models. The partition coefficient approach has broad application in geochemical studies, from metal partitioning between magmatic melts and solids [65], to low-temperature exchange reactions that occur during calcite (re-)crystallization in water [66], and showed promise to explain Sr^{2+} partitioning into siderite ($FeCO_3$) during bacterial ferrihydrite reduction [43]. Extension of this relatively simple model to metal cycling during Fe^{2+}-catalysed iron oxide recrystallization may be of significant use to the geochemistry and engineering communities as an input into predictive and reactive transport models

In addition to uncertainty regarding the mechanism of metal incorporation during Fe^{2+}-catalysed iron oxide recrystallization, it is also unclear whether or not structurally incorporated metals become more or less labile after incorporation. For example, the incorporation of uranium in iron oxides has been suggested to make the uranium less resistant to oxidative mobilization [5,50]. Addressing these questions is critical for implementing water quality management strategies aiming to reduce iron oxides and sequester toxic metals (e.g. [67]), as well as predicting the release of metals such as arsenic into water (e.g. [7,46,56]). Further work is clearly needed in this area to assess whether more environmentally pertinent elements (e.g. uranium, arsenic and chromium) are also rapidly released from iron oxides in the presence of aqueous Fe^{2+}.

Funding

References

1 Cornell, R.M. and Schwertmann, U. (2003) The Iron Oxides: Structure, Properties, Reactions, Occurrences and Uses, 2nd edn, Wiley-VCH, Weinheim
2 Frierdich, A.J., Hasenmueller, E.A. and Catalano, J.G. (2011) Composition and structure of nanocrystalline Fe and Mn oxide cave deposits: implications for trace element mobility in karst systems. Chem. Geol. **284**, 82–96

3 Fitzpatrick, R.W. and Schwertmann, U. (1982) Al-substituted goethite an indicator of pedogenic and other weathering environments in South Africa. Geoderma **27**, 335–347

4 Frierdich, A.J. and Catalano, J.G. (2012) Controls on Fe(II)-activated trace element release from goethite and hematite. Environ. Sci. Technol. **46**, 1519–1526

5 Boland, D.D., Collins, R.N., Payne, T.E. and Waite, T.D. (2011) Effect of amorphous Fe(III) oxide transformation on the Fe(II)-mediated reduction of U(VI). Environ. Sci. Technol. **45**, 1327–1333

6 Gorski, C.A., Handler, R.M., Beard, B.L., Pasakarnis, T., Johnson, C.M. and Scherer, M.M. (2012) Fe atom exchange between aqueous Fe^{2+} and magnetite. Environ. Sci. Technol., doi:10.1021/es204649a

7 Pedersen, H.D., Postma, D. and Jakobsen, R. (2006) Release of arsenic associated with the reduction and transformation of iron oxides. Geochim. Cosmochim. Acta **70**, 4116–4129

8 Hansel, C.M., Benner, S.G. and Fendorf, S. (2005) Competing Fe(II)-induced mineralization pathways of ferrihydrite. Environ. Sci. Technol. **39**, 7147–7153

9 Pedersen, H.D., Postma, D., Jakobsen, R. and Larsen, O. (2005) Fast transformation of iron oxyhydroxides by the catalytic action of aqueous Fe(II). Geochim. Cosmochim. Acta **69**, 3967–3977

10 Yang, L., Steefel, C.I., Marcus, M.A. and Bargar, J.R. (2010) Kinetics of Fe(II)-catalyzed transformation of 6-line ferrihydrite under anaerobic flow conditions. Environ. Sci. Technol. **44**, 5469–5475

11 Tamaura, Y., Ito, K. and Katsura, T. (1983) Transformation of γ-FeO(OH) to Fe_3O_4 by adsorption of iron(II) ion on γ-FeO(OH). J. Chem. Soc., Dalton Trans., 189–194

12 Hansel, C.M., Benner, S.G., Neiss, J., Dohnalkova, A., Kukkadapu, R. and Fendorf, S. (2003) Secondary mineralization pathways induced by dissimilatory iron reduction of ferrihydrite under advective flow. Geochim. Cosmochim. Acta **67**, 2977–2992

13 Stumm, W. (ed.) (1987) Aquatic Surface Chemistry: Chemical Processes at the Particle–Water Interface, Wiley, New York

14 Stumm, W. and Sulzberger, B. (1992) The cycling of iron in natural environments: considerations based on laboratory studies of heterogeneous redox processes. Geochim. Cosmochim. Acta **56**, 3233–3257

15 Charlet, L., Silvester, E. and Liger, E. (1998) N-compound reduction and actinide immobilisation in surficial fluids by Fe(II): the surface Fe(III)OFe(II)OH degrees species, as major reductant. Chem. Geol. **151**, 85–93

16 Liger, E., Charlet, L. and Van Cappellen, P. (1999) Surface catalysis of uranium(VI) reduction by iron(II). Geochim. Cosmochim. Acta **63**, 2939–2955

17 Mikutta, C., Wiederhold, J.G., Cirpka, O.A., Hofstetter, T.B., Bourdon, B. and Von Gunten, U. (2009) Iron isotope fractionation and atom exchange during sorption of ferrous iron to mineral surfaces. Geochim. Cosmochim. Acta **73**, 1795–1812

18 Jang, J.H., Mathur, R., Liermann, L.J., Ruebush, S. and Brantley, S.L. (2008) An iron isotope signature related to electron transfer between aqueous ferrous iron and goethite. Chem. Geol. **250**, 40–48

19 Crosby, H.A., Johnson, C.M., Roden, E.E. and Beard, B.L. (2005) Coupled Fe(II)–Fe(III) electron and atom exchange as a mechanism for Fe isotope fractionation during dissimilatory iron oxide reduction. Environ. Sci. Technol. **39**, 6698–6704

20 Crosby, H.A., Roden, E.E., Johnson, C.M. and Beard, B.L. (2007) The mechanisms of iron isotope fractionation produced during dissimilatory Fe(III) reduction by *Shewanella putrefaciens* and *Geobacter sulfurreducens*. Geobiology **5**, 169–189

21 Wiesli, R.A., Beard, B.L. and Johnson, C.M. (2004) Experimental determination of Fe isotope fractionation between aqueous Fe(II), siderite and "green rust" in abiotic systems. Chem. Geol. **211**, 343–362

22 Johnson, C.M., Roden, E.E., Welch, S.A. and Beard, B.L. (2005) Experimental constraints on Fe isotope fractionation during magnetite and Fe carbonate formation coupled to dissimilatory hydrous ferric oxide reduction. Geochim. Cosmochim. Acta **69**, 963–993

23 Jones, A.M., Collins, R.N., Rose, J. and Waite, T.D. (2009) The effect of silica and natural organic matter on the Fe(II)-catalysed transformation and reactivity of Fe(III) minerals. Geochim. Cosmochim. Acta **73**, 4409–4422

24 Gorski, C.A. and Scherer, M.M. (2011) Fe^{2+} sorption at the Fe oxide–water interface: a revised conceptual framework Aquatic Redox Chemistry (Tratnyek, P.G., Grundl, T.J. and Haderlein, S.B., eds), pp. 315–343, American Chemical Society, Washington, DC

25 Tronc, E., Jolivet, J.-P., Lefebvre, J. and Massart, R. (1984) Ion adsorption and electron transfer in spinel-like iron oxide colloids. J. Chem. Soc., Faraday Trans. **80**, 2619–2629

26 Jeon, B.H., Dempsey, B.A. and Burgos, W.D. (2003) Kinetics and mechanisms for reactions of Fe(II) with iron(III) oxides. Environ. Sci. Technol. **37**, 3309–3315

27 Jeon, B.H., Dempsey, B.A., Burgos, W.D. and Royer, R.A. (2003) Sorption kinetics of Fe(II), Zn(II), Co(II), Ni(II), Cd(II), and Fe(II)/Me(II) onto hematite. Water Res. **37**, 4135–4142

28 Coughlin, B.R. and Stone, A.T. (1995) Nonreversible adsorption of divalent metal-ions (Mn^{II}, Co^{II}, Ni^{II}, Cu^{II}, and Pb^{II}) onto goethite: effects of acidification, Fe^{II} addition, and picolinic-acid addition. Environ. Sci. Technol. **29**, 2445–2455

29 Williams, A.G.B. and Scherer, M.M. (2004) Spectroscopic evidence for Fe(II)–Fe(III) electron transfer at the Fe oxide–water interface. Environ. Sci. Technol. **38**, 4782–4790

30 Gorski, C.A. and Scherer, M.M. (2009) Influence of magnetite stoichiometry on Fe^{II} uptake and nitrobenzene reduction. Environ. Sci. Technol. **43**, 3675–3680

31 Larese-Casanova, P. and Scherer, M.M. (2007) Fe(II) sorption on hematite: new insights based on spectroscopic measurements. Environ. Sci. Technol. **41**, 471–477

32 Catalano, J.G., Fenter, P., Park, C., Zhang, Z. and Rosso, K.M. (2010) Structure and oxidation state of hematite surfaces reacted with aqueous Fe(II) at acidic and neutral pH. Geochim. Cosmochim. Acta **74**, 1498–1512

33 Tanwar, K.S., Petitto, S.C., Ghose, S.K., Eng, P.J. and Trainor, T.P. (2008) Structural study of Fe(II) adsorption on hematite (1 02). Geochim. Cosmochim. Acta **72**, 3311–3325

34 Rosso, K.M., Yanina, S.V., Gorski, C.A., Larese-Casanova, P. and Scherer, M.M. (2010) Connecting observations of hematite (α-Fe_2O_3) growth catalyzed by Fe(II). Environ. Sci. Technol. **44**, 61–67

35 Handler, R.M., Beard, B.L., Johnson, C.M. and Scherer, M.M. (2009) Atom exchange between aqueous Fe(II) and goethite: an Fe isotope tracer study. Environ. Sci. Technol. **43**, 1102–1107

36 Frierdich, A.J., Luo, Y. and Catalano, J.G. (2011) Trace element cycling through iron oxide minerals during redox driven dynamic recrystallization. Geology **39**, 1083–1086

37 Yanina, S.V. and Rosso, K.M. (2008) Linked reactivity at mineral-water interfaces through bulk crystal conduction. Science **320**, 218–222

38 Bruemmer, G.W., Gerth, J. and Tiller, K.G. (1988) Reaction kinetics of the adsorption and desorption of nickel, zinc and cadmium by goethite. I. Adsorption and diffusion of metals. J. Soil Sci. **39**, 37–52

39 Mikutta, C., Lang, F. and Kaupenjohann, M. (2006) Citrate impairs the micropore diffusion of phosphate into pure and C-coated goethite. Geochim. Cosmochim. Acta **70**, 595–607

40 Fischer, L., Brummer, G.W. and Barrow, N.J. (2007) Observations and modelling of the reactions of 10 metals with goethite: adsorption and diffusion processes. Eur. J. Soil Sci. **58**, 1304–1315

41 Putnis, A. (2002) Mineral replacement reactions: from macroscopic observations to microscopic mechanisms. Mineral. Mag. **66**, 689–708

42 Fredrickson, J.K., Zachara, J.M., Kukkadapu, R.K., Gorby, Y.A., Smith, S.C. and Brown, C.F. (2001) Biotransformation of Ni-substituted hydrous ferric oxide by an Fe(III)-reducing bacterium. Environ. Sci. Technol. **35**, 703–712

43 Roden, E.E., Leonardo, M.R. and Ferris, F.G. (2002) Immobilization of strontium during iron biomineralization coupled to dissimilatory hydrous ferric oxide reduction. Geochim. Cosmochim. Acta **66**, 2823–2839

44 Coker, V.S., Pearce, C.I., Pattrick, R.A.D., Van Der Laan, G., Telling, N.D., Charnock, J.M., Arenholz, E. and Lloyd, J.R. (2008) Probing the site occupancies of Co-, Ni-, and Mn-substituted biogenic magnetite using XAS and XMCD. Am. Mineral. **93**, 1119–1132

45 Roh, Y., Lauf, R.J., Mcmillan, A.D., Zhang, C., Rawn, C.J., Bai, J. and Phelps, T.J. (2001) Microbial synthesis and the characterization of metal-substituted magnetites. Solid State Commun. **118**, 529–534

46 Coker, V.S., Gault, A.G., Pearce, C.I., Van Der Laan, G., Telling, N.D., Charnock, J.M., Polya, D.A. and Lloyd, J.R. (2006) XAS and XMCD evidence for species-dependent partitioning of arsenic during microbial reduction of ferrihydrite to magnetite. Environ. Sci. Technol. **40**, 7745–7750

47 O'Loughlin, E.J., Gorski, C.A., Scherer, M.M., Boyanov, M.I. and Kemner, K.M. (2010) Effects of oxyanions, natural organic matter, and bacterial cell numbers on the bioreduction of lepidocrocite (γ-FeOOH) and the formation of secondary mineralization products. Environ. Sci. Technol. **44**, 4570–4576

48 Jang, J.H., Dempsey, B.A., Catchen, G.L. and Burgos, W.D. (2003) Effects of Zn(II), Cu(II), Mn(II), Fe(II), NO_3^-, or SO_4^{2-} at pH 6.5 and 8.5 on transformations of hydrous ferric oxide (HFO) as evidenced by Mossbauer spectroscopy. Colloids Surf., A **221**, 55–68

49 Anthony, J.W., Bideaux, R.A., Bladh, K.W. and Nichols, M.C. (1990) Handbook of Mineralogy, Mineral Data Publishing, Tucson

50 Nico, P.S., Stewart, B.D. and Fendorf, S. (2009) Incorporation of oxidized uranium into Fe (hydr)oxides during Fe(II) catalyzed remineralization. Environ. Sci. Technol. **43**, 7391–7396

51 Wu, L., Beard, B.L., Roden, E.E. and Johnson, C.M. (2011) Stable iron isotope fractionation between aqueous Fe(II) and hydrous ferric oxide. Environ. Sci. Technol. **45**, 1847–1852

52 Jeon, B.H., Dempsey, B.A., Burgos, W.D. and Royer, R.A. (2001) Reactions of ferrous iron with hematite. Colloids Surf., A **191**, 41–55

53 Cutting, R.S., Coker, V.S., Telling, N.D., Kimber, R.L., Pearce, C.I., Ellis, B.L., Lawson, R.S., Van Der Laan, G., Pattrick, R.A.D., Vaughan, D.J. et al. (2010) Optimizing Cr(VI) and Tc(VII) remediation through nanoscale biomineral engineering. Environ. Sci. Technol. **44**, 2577–2584

54 Beard, B.L., Handler, R.M., Scherer, M.M., Wu, L., Czaja, A.D., Heimann, A. and Johnson, C.M. (2010) Iron isotope fractionation between aqueous ferrous iron and goethite. Earth Planet. Sci. Lett. **295**, 241–250

55 Um, W., Chang, H.S., Icenhower, J.P., Lukens, W.W., Serne, R.J., Qafoku, N.P., Westsik, J.H., Buck, E.C. and Smith, S.C. (2011) Immobilization of 99-technetium(VII) by Fe(II)-goethite and limited reoxidation. Environ. Sci. Technol. **45**, 4904–4913

56 Catalano, J.G., Luo, Y. and Otemuyiwa, B. (2011) Effect of aqueous Fe(II) on arsenate sorption on goethite and hematite. Environ. Sci. Technol. **45**, 8826–8833

57 Zachara, J.M., Fredrickson, J.K., Smith, S.C. and Gassman, P.L. (2001) Solubilization of Fe(II) oxide-bound trace metals by a dissimilatory Fe(II) reducing bacterium. Geochim. Cosmochim. Acta **65**, 75–93

58 Bousserrhine, N., Gasser, U.G., Jeanroy, E. and Berthelin, J. (1999) Bacterial and chemical reductive dissolution of Mn-, Co-, Cr-, and Al-substituted goethites. Geomicrobiol. J. **16**, 245–258

59 Cooper, D.C., Picardal, F.F. and Coby, A.J. (2006) Interactions between microbial iron reduction and metal geochemistry: effect of redox cycling on transition metal speciation in iron bearing sediments. Environ. Sci. Technol. **40**, 1884–1891

60 Hansel, C.M., Learman, D.R., Lentini, C.J. and Ekstrom, E.B. (2011) Effect of adsorbed and substituted Al on Fe(II)-induced mineralization pathways of ferrihydrite. Geochim. Cosmochim. Acta **75**, 4653–4666

61 Kerisit, S., Felmy, A.R. and Ilton, E.S. (2011) Atomistic simulations of uranium incorporation into iron (hydr)oxides. Environ. Sci. Technol. **45**, 2770–2776

62 Skomurski, F.N., Rosso, K.M., Krupka, K.M. and Mcgrail, B.P. (2010) Technetium incorporation into hematite (α-Fe2O3). Environ. Sci. Technol. **44**, 5855–5861

63 Henderson, L.M. and Kracek, F.C. (1927) The fractional precipitation of barium and radium chromates. J. Am. Chem. Soc. **49**, 738–749

64 Doerner, H.A. and Hoskins, W.M. (1925) Co-precipitation of radium and barium sulfates. J. Am. Chem. Soc. **47**, 662–675

65 Beattie, P., Ford, C. and Russell, D. (1991) Partition coefficients for olivine-melt and orthopyroxene-melt systems. Contrib. Mineral. Petrol. **109**, 212–224

66 Temmam, M., Paquette, J. and Vali, H. (2000) Mn and Zn incorporation into calcite as a function of chloride aqueous concentration. Geochim. Cosmochim. Acta **64**, 2417–2430

67 O'Loughlin, E.J., Boyanov, M.I., Antonopoulos, D.A. and Kemner, K.M. (2011) Redox processes affecting the speciation of technetium, uranium, neptunium, and plutonium in aquatic and terrestrial environments. In Aquatic Redox Chemistry (Tratnyek, P.G., Grundl, T.J. and Haderlein, S.B., eds), pp. 477–517, American Chemical Society, Washington, DC

68 Schwertmann, U. and Cornell, R.M. (2000) Iron Oxides in the Laboratory: Preparation and Characterization, 2nd edn, Wiley-VCH, Weinheim

69 Tamura, H., Goto, K., Yotsuyan, T. and Nagayama, M. (1974) Spectrophotometric determination of iron(II) with 1,10-phenanthroline in presence of large amounts of iron(III). Talanta **21**, 314–318

70 Morgan, J.J. and Stumm, W.S. (1965) Analytical chemistry of aqueous manganese. J. Am. Water Works Assoc. **57**, 107–119

71 Shannon, R.D. (1976) Revised effective ionic radii and systematic studies of interatomic distances in halides and chalcogenides. Acta Crystallogr. Sect. A Cryst. Phys. Diffr. Theor. Gen. Crystallogr. **32**, 751–767